# 3D WAVE PROPAGATION MODELING OF THE 12 05 2008 SICHUAN Ms 7.9 EARTHQUAKE

**M. Chavez[1,2], E. Cabrera[3], H. Chen[4], N. Perea[1], A. Salazar[3], D. Emerson[5]**
**M. Ashworth[5], Ch. Moulinec[5], M. Wu[4], G. Zhao[4]**

[1] Institute of Engineering, UNAM, C.U., 04510, Mexico DF, Mexico
[2] Laboratoire de Géologie CNRS-ENS, 24 Rue Lhomond, Paris, France
[3] DGSCA, UNAM, C.U., 04510, Mexico DF, Mexico
[4] C E N C, 63 Fuxing Rd., Beijing, 100036, P.R.China
[5] STFC Daresbury Laboratory, Warrington WA4 4AD, UK

## ABSTRACT

The seismic potential of southern China is associated to the continent-continent collision between the Indian and the Eurasian plates, this is manifested in the Western Sichuan Plateau (eastern Tibetan Plateau) by several, seismically active system of faults, such as the Longmenshan fault. The seismicity observed on the latter includes recent historical events with magnitudes up to 6.5, and the one of the 12 05 2008 Ms 7.9 (Mo 1.15 $10^{28}$ dyne/cm) thrust mechanism, so-called Sichuan earthquake. In this work, a hybrid procedure, combining long period and high frequency simulations (which for the low frequencies computations includes a recently optimized 3D seismic wave propagation parallel finite difference code) was used to obtain 3D synthetics seismograms for the mentioned Sichuan earthquake. The modeling included the USGS web-site, 40 x 315 $km^2$ kinematic description of the earthquake´s rupture. The comparisons between observed and synthetic seismograms for stations sites of the Seismological Network of China, such as CD2 (Chengdu), GYA, LHZ and TIY at about 90, 500, 600 and 1200 Km from the epicenter of the Sichuan event, respectively, are satisfactory. Maximum synthetic accelerations, velocities and displacements, and permanent displacements of: 1.70 $m/s^2$ , 1.90 m/s, 3.30 m, and 1.25 m; and 0.625 $m/s^2$ , 0.092 m/s, 0.10 m, and 0.0 m, were obtained for (assuming rock sites) Beichuan and Chengdu, respectively, which partially explains the modification of the topography, and the extensive damage observed on the infrastructure and towns located on top of the Sichuan earthquake rupture zone, as well as the slight damage observed at Chengdu located at an epicentral distance of 90 km.

**KEYWORDS: Observations, 3D modeling, finite differences, earthquake, Sichuan.**

## 1. INTRODUCTION

The seismic potential of southern China is associated to the continent-continent collision between the Indian and the Eurasian plates. The mentioned collision is manifested in the Western Sichuan Plateau (eastern Tibetan Plateau) in central-southern China, by several, seismically active system of faults, such as the Longmenshan fault system, where the epicenter of the very damaging (about 70,000 deaths and 100 billion US dollars loss) 12 05 2008 Ms 7.9 Sichuan earthquake is located. In this work, a hybrid procedure, combining long period and high frequency simulations, which was successfully utilized to model the wave propagation of the 09/10/1995 Ms 7.6 Colima-Jalisco earthquake (Chavez et al., 2004), was utilized for the computation of broadband synthetics seismograms for the Sichuan earthquake. For the low frequency synthetics, a recently optimized 3D seismic wave propagation parallel finite difference code (Cabrera and Chavez et al, 2007) was used to obtain 3D velocities synthetics in the region of interest. The supercomputers KanBalam (Mexico) and HECToR (UK) were used to run the code.

The paper is divided in 6 parts. In the 2nd we discuss the main seismotectonic features of southern China; In the 3rd a brief discussion of the 3D hybrid modeling procedure is included; the characteristics of some of the recordings observed for the 12 05 2008 Ms 7.9 Sichuan earthquake and its aftershocks are presented in the 4th , and the data and numerical results of the modeling for the Sichuan earthquake are presented in the 5th. Finally the main conclusions of the work are presented.

## 2. SEISMO AND GEO TECTONIC FEATURES OF CENTRAL SOUTHERN CHINA

The seismotectonic characteristics of the central-southern China region are mainly associated with the collision between the Indian and the Eurasian plates. Among other manifestation of the mentioned collision, recent Global Positioning System (GPS) measurements of crustal motion in the central eastern Tibetan Plateau and its adjacent foreland indicates a shortening of about 3mm/year within the Longmenshan region. This region is located between the Western Sichuan Plateau and the Sichuan Basin, Fig 1. The latter is part of the Yangtze Craton, and Wang et al., (2007) proposed that the collision between this and the Tibetan Plateau have produced the thickening of the lower crust and the uplift of the western Sichuan Plateau. Another expression of the mentioned collision, is the seismicity in the region, which includes the occurrence of earthquakes with magnitudes ≤ 6.5 on the Longmenshan fault system (and of up to 8 in its vicinity, at least since 1879) until the one with a Ms 7.9 of the 12/05/2008, as shown in Fig. 1. Notice in this figure, that the surface projection of its rupture area was of about 30 x 315 km$^2$, and that its largest kinematic slips (up to 9 m, Fig. 5), represented by three inner rectangles of its rupture area, are located between and off the two concentration of events with magnitudes ≤ 6.5, occurred from 1960-2007, identified by open circles inside the shaded ellipsoids, Fig. 1.

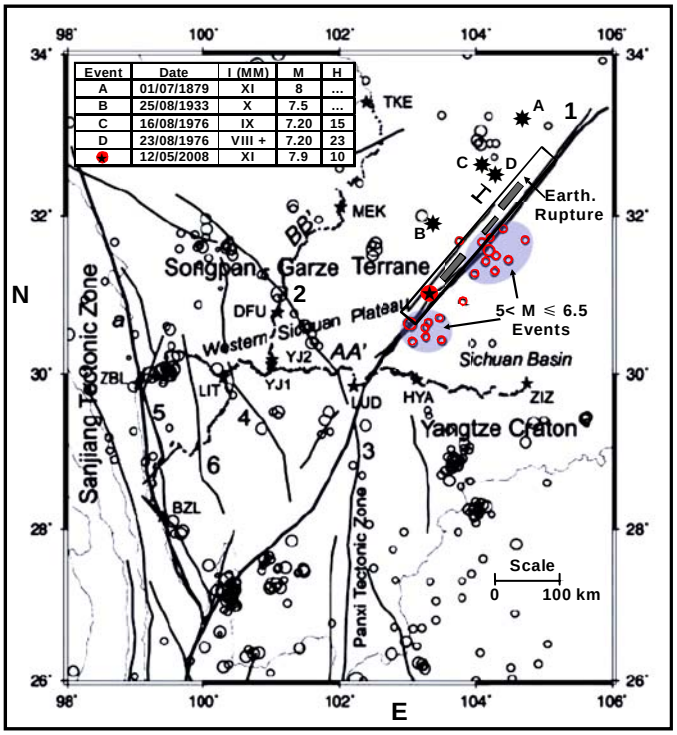


Fig. 1 Fault systems in the region of interest are identified by numbers, 1 is the Longmenshan system. Open circles denote the epicenters of earthquakes with magnitudes > 5 occurred from 1960 to 2007. The epicenters of M ≥ 7.2 earthquakes are identified with the letters A to D (Modif. Wang et al., 2007). The surface projection of the rupture area of the 12 05 2008 Ms 7.9 Sichuan earthquake is represented by the long rectangle, and its inner black rectangles identify the areas with kinematic slips > 7 to 9 m (Modif. USGS site, 2008).

With respect to the structural geotectonic characteristics of the region of interest, recently, Li et al. (2006) proposed 14 crustal models for mainland China. Those models are the result of about 90 seismic refraction/wide angle reflection profiles and include representative crustal seismic velocity (of compressional waves, Vp) - depth columns, associated to the 14 tectonic units of China proposed by Huang et al. (1980, cited by Li et al., 2006).

Wang et al. (2007) performed active source seismic refraction and wide angle reflection (i.e., Deep Seismic Sounding) experiments in the Western Sichuan Plateau and the Sichuan Basin region. From those experiments they obtained seismic profiles in the cited region, which led them to propose the 3D geotectonic structure shown in Fig. 2, as well as the corresponding compressional velocity (Vp) and densitiy models.

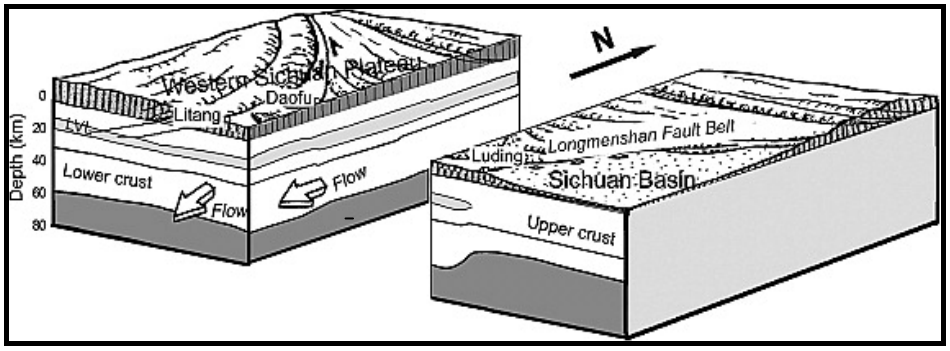


Fig. 2 3D diagram of the crustal kinematic model for the eastern margin of the Tibetan Plateau, constructed from 2-D crustal structures (Modified, Wang et al., 2007).

The variation of the shear wave velocity, Vs, with depth for the Sichuan region was recently obtained by Xu et al. (2008). They applied the receiver function technique to Very Broad Band recordings of teleseismic earthquakes in 25 temporal stations, disseminated in the Sichuan region. Among other results, they included the Vs crustal velocities up to a depth of 80 km for sites located in the vicinity of the Longmenshan fault system. Of particular interest for this work is their finding, that on the first 7 km depth, the Vs values are smaller than 3 km/s, Xu et al. (2008) also proposed ratios of Vp/Vs for those stations, which, on average are equal to 1.86 + - 0.07.

## 3. BROADBAND HYBRID MODELING PROCEDURE

A hybrid procedure (Fig. 3), combining long period and high frequency simulations (Chavez et al., 2004) was utilized for the computation of broadband synthetic seismograms for the Ms 7.9 of the 12/05/2008 Sichuan earthquake. The long period (< 0.3 Hz) wave field was simulated using a recently optimized 3D seismic wave propagation parallel finite difference code, that uses 2nd order operators in time and 4th order differences in space (Cabrera and Chavez et al, 2007). The high frequency (≥ 0.3Hz) synthetics were generated with the Empirical Green function (EGF) method, Irikura (1986). In this method the ground motion of a large event is expressed as the superposition of the records of small events (elementary sources). Finally, the low and high frequency synthetics are combined using matched filters (Chavez et al., 2004).

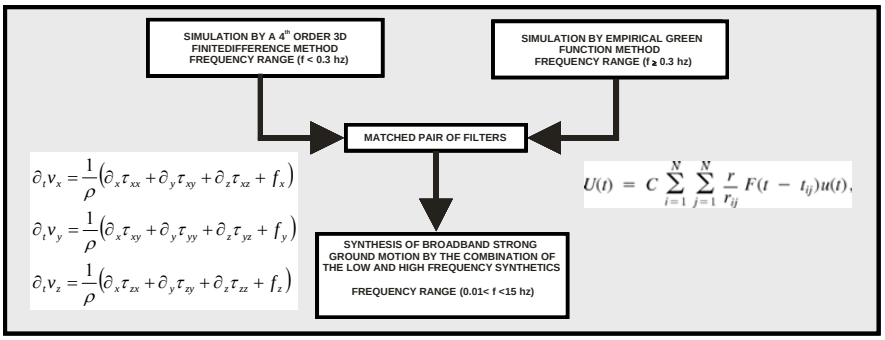


Fig. 3 Hybrid procedure combining long period and high frequency simulations (Chavez et al., 2004)

## 4. OBSERVATION OF THE 12 05 2008 Ms 7.9 SICHUAN EARTHQUAKE AND SOME OF ITS AFTERSHOCKS

In Fig. 4, examples of the velocity seismograms (and of their associated Fourier amplitude spectra) recorded for the Ms 7.9 mainshock and its (in this case Ms 6) aftershocks, at CD2 (Chengdu) located at about 90 km of the

the epicenters of the both events, are presented. Notice in Fig. 4A, that for the observations of the Ms 7.9 main shock, the records at CD2 station are saturated, i.e., the maximum amplitudes of the ground motion velocities could not be recorded, because the Very Broad Band seismographs of the Seismological Network of China (SNC), reached their maximum range. However, this was not the case for the records of the Ms 6 aftershock. Similar observations can be made (Chavez et al, in preparation) for the recordings at other SNC stations, such as GYA, LZH and TIY located at about 500, 650 and 1300 km from the epicenter of the mainshock (Fig. 5).

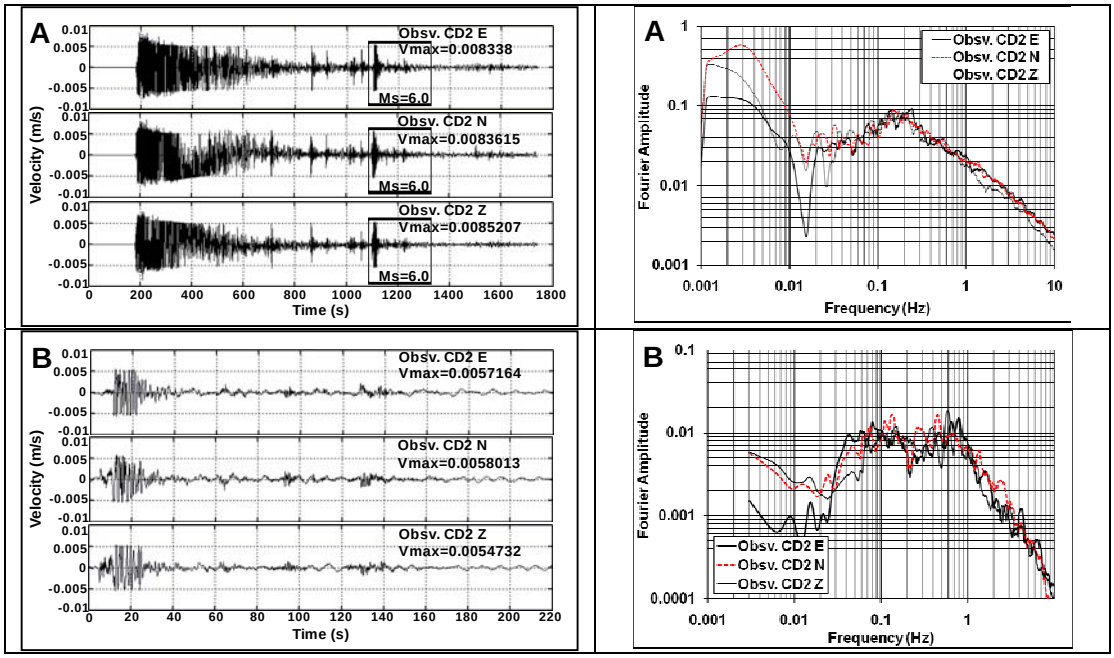


Fig. 4 Velocity seismograms in the East (E), North (N) and vertical (Z) directions observed at station CD2 (Chengdu), and their corresponding Fourier Amplitude spectra, for the: A) 12 05 2008 Ms 7.9 Sichuan earthquake and B) its Ms 6 aftershock of the same day.

## 5. 3D MODELING OF THE WAVE PROPAGATION OF THE 12 05 2008 SICHUAN MS 7.9 EARTHQUAKE

The hybrid procedure described in part 3 was utilized for the computation of broadband synthetic seismograms for the Ms 7.9 of the 12/05/2008 Sichuan earthquake. In Fig 5, the surface projection of the 2400(length) x 1600(width) x 300(depth) $km^3$ volume used for the low frequency modeling of the Sichuan earthquake is presented. The same figure includes the kinematic slip distribution adopted for the event. The parameters utilized in the modeling are shown in Table 1.

To obtain the low frequency synthetic seismograms for the event of interest, it is necessary to propose a model to represent the geological structure of the volume whose surface projection is depicted in Fig. 5, this was done here by considering the structural geotectonic information depicted in Fig 2, and the studies synthesized in part 2. Therefore, as a first approach to the modeling of the geologic structure for the region of interest depicted in Fig. 5, the geologic column shown in this figure is adopted here for the variation with depth of: the thickness, Vp, Vs and the densities of the different geological layers included in this column. Notice that a trade off on all of those properties was performed, favoring the values corresponding to the Longmenshan fault system and the Sichuan Basin zones where the rupture of the 12 05 2008 Ms 7.9 Sichuan earthquake took place, i.e. where the seismic source from which the seismic waves radiated throughout the 3D domain of interest (Chavez et al, in preparation). The computation of the low frequency synthetics was performed on the supercomputers KanBalam (Mexico) and HECToR (UK).

For the high frequency modeling, the recordings of aftershocks, as the one shown in Fig. 4, for the different SNC stations (Fig. 5) were used. The adopted elementary sources corresponded to the areas with kinematic slips larger than 5 m (Fig. 5), (Chavez et al, in preparation).

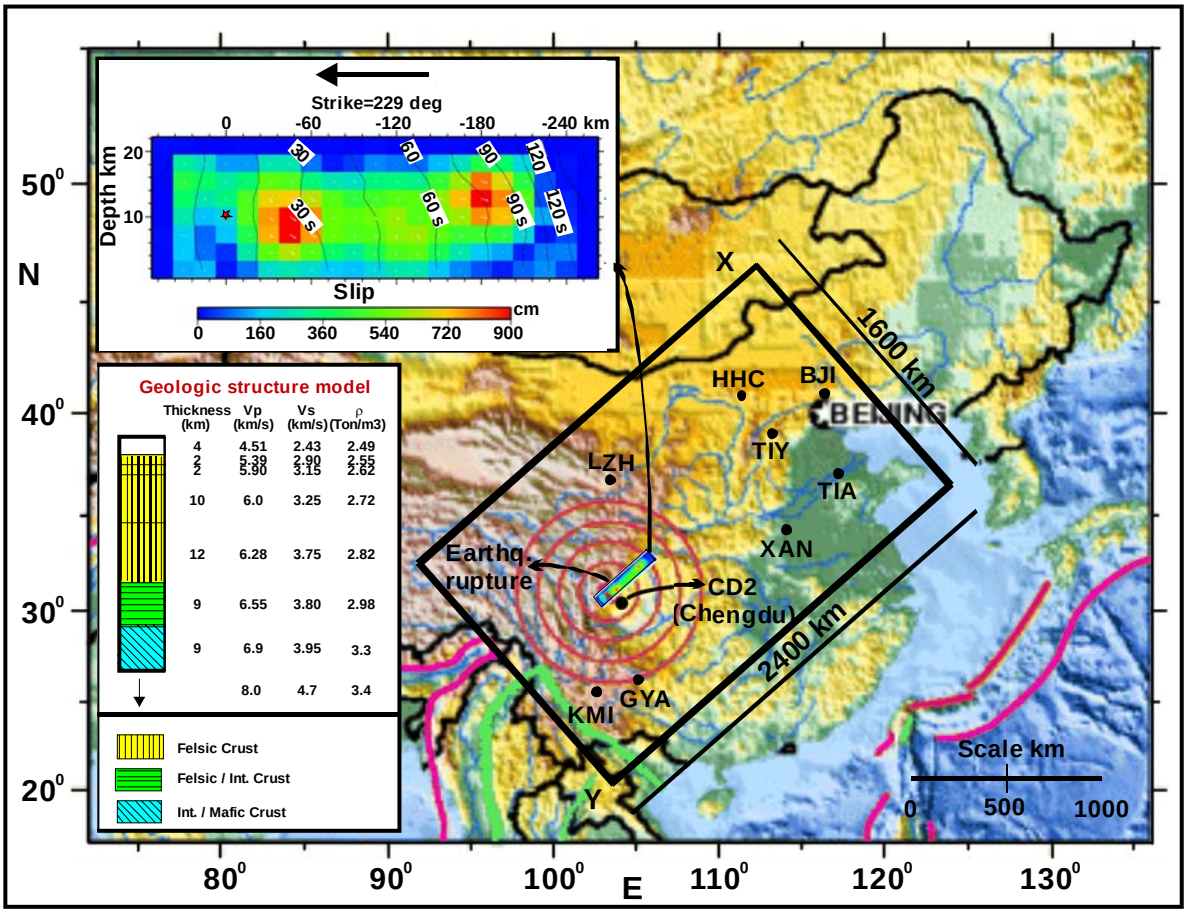


Fig. 5 Locations of: a) the epicenter (red dot) of the 12 05 2008 Sichuan Ms 7.9; b) its rupture area and its kinematic slip; c) 9 seismographic stations sites (black dots) of the China Seismographic Network; d) the surficial projection of the 2400 x 1600 x 300 km$^3$ volume used to discretize the region of interest; f) the geologic structure adopted for the volume. (Modified from USGS web site, 2008).

Table 1. Parameters for the 3D low frequency modeling

| Parameters | Value |
|---|---|
| Spatial discretization (km) | 1.0 |
| Temporal discretization (s) | 0.03 |
| P wave minimum velocity (km/s) | 4.5 |
| S wave minimum velocity (km/s) | 2.4 |
| Minimum density (Ton/m$^3$) | 2.5 |
| Number of grid points X direction | 2400 |
| Number of grid points Y direction | 1600 |
| Number of grid points vertical direction | 300 |
| Number of the time steps | 20000 |
| Simulation time (s) | 600 |

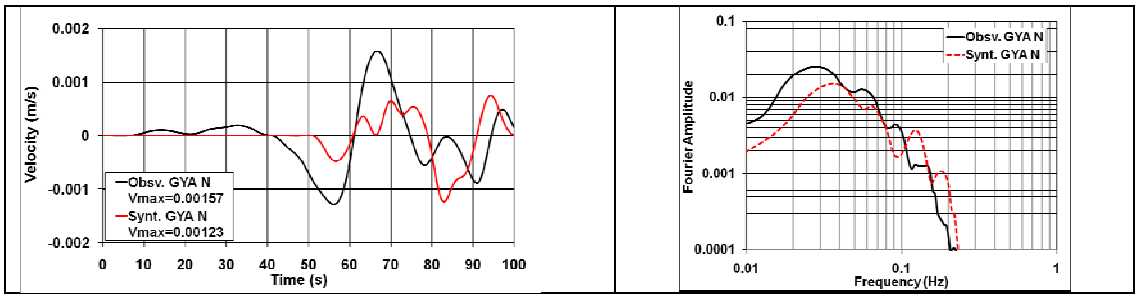


Fig. 6 Observed and (low frequency) synthetic velocity seismograms in the North (N) direction for station GYA (Fig. 5), and its respective Fourier amplitude spectra for the 12 05 2008 Sichuan Ms 7.9 earthquake.

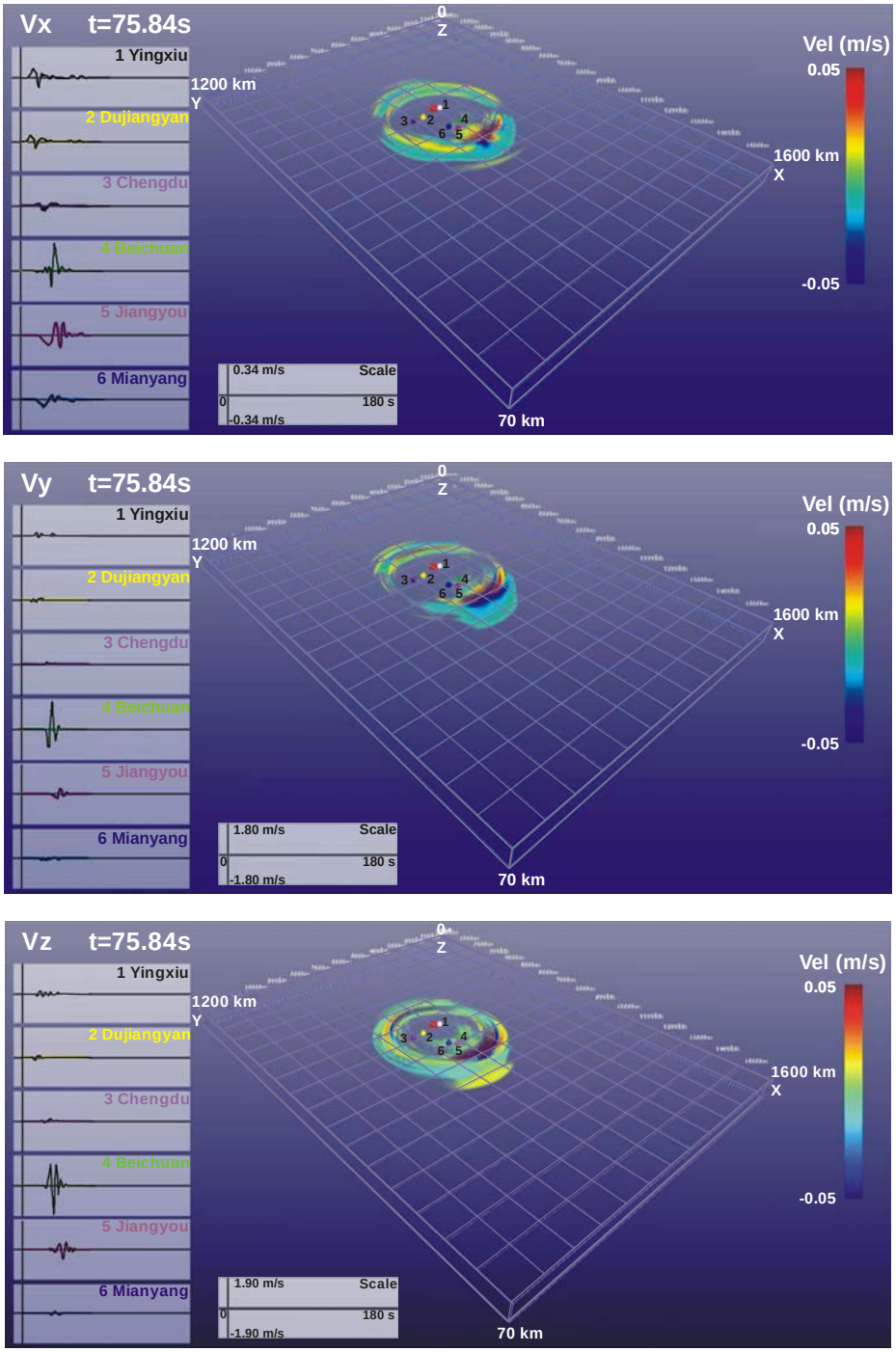


Fig. 7 3D Snapshots (at t = 75.84 s) of the synthetic velocities wavefields (f < 0.3 Hz) in the X, Y and Z directions (Fig. 5), for the 12 05 2008 Ms 7.9 Sichuan earthquake modeling. Also, the 3D synthetic velocity seismograms computed for Yinxiu, Dujiangyan, Chengdu (CD2 station), Beichuan, Jiangyou and Mianyang.

As the main objective of this work is the 3D modeling of the wave propagation generated by the 12 05 08 Sichuan mainshock and compare the synthetic seimograms with observations, in Fig. 6, an example of the type of results obtained is presented. In this figure, the observed and (low frequency) synthetic velocity seismograms in the North (N) direction for station GYA (Fig. 5), and its respective Fourier amplitude spectra are shown. Notice that in general, the comparison of the shapes and the amplitudes, in both the time and frequency domains are satisfactory, for lack of space, other results will be presented elsewhere (Chavez et al, in preparation).
In Fig. 7, 3D Snapshots (at t = 75.84 s) of the synthetic velocities wavefields (f < 0.3 Hz) in the X, Y and Z directions (Fig. 5), obtained for the 12 05 2005 Ms 7.9 Sichuan earthquake modeling are shown. Also, in this

figure, the low frequency, 3D synthetic velocity seismograms computed for Yinxiu (1), Dujiangyan (2), Chengdu (CD2 station) (3), Beichuan (4), Jiangyou (5) and Mianyang (6), are presented. From the snapshots results, the following observations can be made: a) the largest amplitudes in the X, Y and Z wavefields occurred in the positive X direction, which was the rupture direction of the Sichuan earthquake reported by the USGS web site (2008); b) the smaller amplitudes in the X, Y wavefields, occurred in a coned shaped volume generated by a 30 (for the X wavefield) to 60 (for the Y wavefield) degrees, roughly in the Y direction.

With respect to the low frequency synthetic velocity seismograms (on rock site conditions) of Fig. 7, notice that for the X direction, the largest amplitudes occurred at Beichuan (about 0.30 m/s), followed by Jiangyou, Yinxiu, Dujiangyan, Mianyang and Chengdu, which has the minimum amplitude. For the Y and Z directions, a similar trend is observed, with the maximum amplitude of about 1.8 and 1.9 m/s for Beichuan in the Y and Z directions, respectively.

In Fig. 8 A, the low frequency synthetic accelerograms for Beichuan (rock site conditions) are presented. The maximum values are of 0.26, 1.54 and 1.63 m/s$^2$ for the X, Y and Z direction respectively. Incidentally, a maximum horizontal acceleration of about 4.22 m/s$^2$ in the E direction, was observed for the Sichuan earthquake, at an accelerographic station site, nearby Beichuan, resting on soil conditions (X. Li, personal communication) i.e. about 2.74 times the synthetic value in the Y direction on a rock condition. Therefore, we can conclude that the computed synthetic values are reasonable. In Fig. 8B, the acceleration response spectra corresponding to the accelerograms of Fig 8A are shown. Notice that the maximum amplitudes of the former, are of about 5 and 6 m/s$^2$ and occur at periods of 5 and 6 s for the Y and Z directions, respectively. Finally, in Fig. 9, as an example of the type of broadband synthetics obtained in the study (Chavez et al. in preparation), the synthetic seismograms and their respective Fourier amplitude spectra of acceleration, velocity and displacement in the E direction, for Chengdu (station CD2 of the SNC on rock conditions) are presented. From Fig. 9 it can be concluded that maximum synthetic accelerations, velocities and displacements, and permanent displacements of 0.625 m/s$^2$ , 0.092 m/s, 0.10 m, and 0.0 m were computed for the Chengdu site. It is convenient to mention that a maximum horizontal acceleration of about 0.8 m/s$^2$ was observed at Chengdu on a rock condition site for the Sichuan earthquake (X. Li, personal communication).

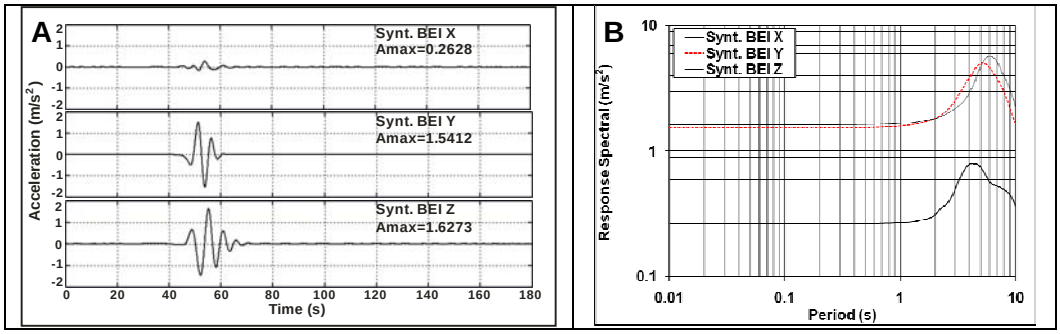


Fig. 8 A) Low frequency synthetic accelerograms in the X, Y and Z directions (Fig. 5) for Beichuan for the 12 05 2008 Ms 7.9 Sichuan earthquake modeling and B) their corresponding acceleration response spectra.

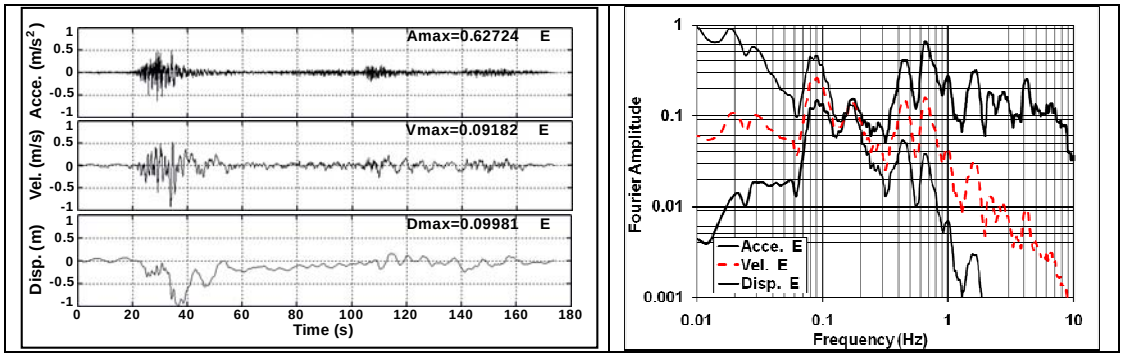


Fig. 9 Broadband synthetic seismograms of acceleration, velocity and displacement, in the E direction for station CD2 (Chengdu, on a rock site, Fig. 5) for the 12 05 2008 Ms 7.9 Sichuan earthquake modeling and its corresponding Fourier amplitude spectra.

## 6. CONCLUSIONS

In this work, a hybrid procedure combining long period and high frequency simulations (which for the low frequencies computations includes a recently optimized 3D seismic wave propagation parallel finite difference code) was used to obtain 3D synthetics seismograms for the 12 05 2008 Ms 7.9 Sichuan earthquake. The synthetics were obtained on the surface projection of a volume of 2400 x 1600 x 300 $km^3$, the volume included the 40 x 315 $km^2$ kinematic description of the earthquake´s rupture. The spatial and temporal modeling discretizations were of 1 km and 0.03 s, respectively. The comparisons between the observed and the synthetic seismograms for stations sites of the Seismological Network of China, such as CD2 (Chengdu) at the epicentral region, GYA at about 600 km and TIY at about 1200 Km from the epicenter, are satisfactory, both in time and frequency domains. Maximum synthetic accelerations, velocities and displacements, and permanent displacements of: 1.70 $m/s^2$ , 1.80 m/s, 3.30 m, and 1.25 m; and 0.625 $m/s^2$ , 0.092 m/s, 0.10 m, and 0.0 m, were obtained for (assuming rock sites) Beichuan and Chengdu, respectively, which partially explains the modification of the topography, and the extensive damage observed on the infrastructure and towns located on top of the Sichuan earthquake rupture zone, as well as the slight damage observed at Chengdu, located at an epicentral distance of 90 km.

## REFERENCES

Cabrera E., M. Chavez, R. Madariaga, N. Perea, M. Frisenda, (2007). Parallel elastodynamic modeling of large subduction earthquakes. F. Capello et al. (eds): Euro PVM/MPI 2007, LNCS 4757, pp. 373-380, Springer-Verlag Berlin Heidelberg.

Chavez M., K. Olsen, E. Cabrera, (2004). Broadband modeling of strong ground motions for prediction purposes for subduction earthquakes occurring in the Colima-Jalisco region of Mexico. 13WCEE, Vancouver, B.C., Canada, August 1-6, Paper No 1653.

Irikura K., (1986). Prediction of strong acceleration motion using empirical Green´s function. Proc. 7th JEES, 151-156.

Li, S., W. D. Mooney, J. Fan, (2006). Crustal structure of mainland China from deep seismic sounding data, Tectonophysics **420**, 239-252.

Wang, C.-Y.,W.-B. Han, J.-P. Wu, H. Lou, and W.W. Chan, (2007). Crustal structure beneath the eastern margin of the Tibetan Plateau and its tectonic implications, J. Geophys. Res., **112**, B07307, doi: 10.1029/2005JB003873.

Xu, L., S. Rondenay, R.D., Van der Hilst, (2008). Structure of the crust beneath the southeastern Tibetan plateau from teleseismic receiver functions. Accepted, Physics of the Earth and Planetary Interiors.

## ACKNOWLEDGMENTS

We acknowledge the support of R. Madariaga of the ENS, Paris. We would like to thank the support of J.L. Gordillo, the Supercomputing staff and M. Ambriz, of DGSCA, and the Institute of Engineering, UNAM, respectively. We acknowledge DGSCA, UNAM for the support to use KanBalam, as well as the STFC Daresbury Laboratory to use HECToR Supercomputers. The authors also acknowledge support from the Scientific Computing Advanced Training (SCAT) project through Europe Aid contract II-0537-FC-FA (http://www.scat-alfa.eu).